THE LIFT AND PITCHING MOMENT CHARACTERISTICS OF AN AIRFOIL IN ISOLATED AND TANDEM CASES

M. A. Yukselen
Istanbul Technical University, Faculty of
Aeronautics And Aerospace,
Istanbul, Turkey

Abstract

Although many problems of the airfoils at medium and high Reynolds numbers are solved, the number of investigations at Reynolds numbers below 10^6 is very limited. In this paper, the lift and pitching moment characteristics of an airfoil in isolated and tandem case are investigated experimentally at a Reynolds number of about 6.5 10^5 and theoretically for the potential case. In the theoretical part, a new panel method, developed in the complex plane starting from the Cauchy integral theorem is presented. The method is applicable also for the cases containing the ground effect or the wind tunnel wall effects. In the experimental part the lift and pitching moment characteristics of a NACA airfoil model are obtained by integrating the measured surface pressure distributions. The wind tunnel wall effects are corrected by using the panel method developed in the complex plane. Experimental results are compared with the theoretical results obtained by the complex panel method and with the published experimental results at Reynolds number of 3 million. These comparisons show the viscosity and Reynolds number effects in isolated case. In the tandem case, the same model is installed in the wake of a similar airfoil model. And the effects of the angles of attack and the distance between the airfoils are investigated.

Introduction

The chord based Reynolds numbers below 10^6 for airfoils are generally accepted as the low Reynolds numbers. This type of flows exist for jet engine compressor and turbine blades, gliders and sailplanes at low speeds, remotely piloted vehicles (RPVs) at high altitudes, ultra light man-carrying/man-powered recreational air-crafts, wind turbines/propellers and new generation ships with wing-sails. Although many problems of the airfoils at medium and high Reynolds numbers are solved, the number of investigations at low Reynolds numbers is very limited. But the current desire to improve the performance of both military and civilian systems has focused attention on this flow regime, in the recent years.[1]

For most of the aerodynamic investigations, it is common to accept the airfoils in uniform-parallel free-flow. In certain cases, however, the flow exerted by the airfoil cannot be considered uniform. Some examples of this type of flows are atmospheric boundary layer flow for a wing during the take off or landing of an aeroplane; propeller wake for some part of a wing; wing wake for tail surfaces. In each cases, the flow approaching to the airfoil is called shear flow, and an extra effect of the velocity gradient in the shear flow is expected on the airfoil performances. There are some other examples in which the velocity gradient or shear flow effect is combined with the potential effect of the body creating the wake and the body taking place in the wake, like a slat-wing-flap combination or a tandem combination.

The effect of a uniform shear flow on an airfoil was first investigated by Tsien[2], in connection with the influence of atmospheric boundary layer. He considered a symmetrical Joukowsky airfoil in an inviscid flow with a uniform shear (Fig.1) and calculated the exact forces and moments on the airfoil by using the conform transformation technique. This work was extended to the cambered Joukowsky airfoils by Sowyrda.[3] In both investigations the effect of a uniform positive shear layer (linearly increasing velocity in the direction of the positive lift) is seen as an increase in the slope of the lift and moment curves like an increasing thickness effect, an overall increase in lift like an increasing camber effect, and an increase in pitching moment like a distortion effect in the camber distribution.

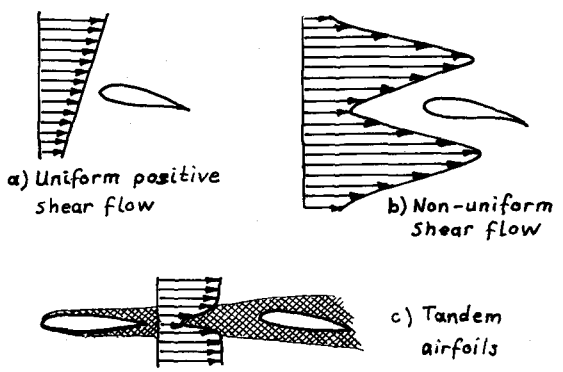

Figure 1 : Examples of shear flow

Several experiments were carried out by Vidal[4], Ludwig and Erickson[5] and Gupta and Sharma[6] on symmetrical and cambered Joukowsky airfoils immersed in non-uniformly sheared flows simulating a propeller wake. The results of these experiments are in the sense to agree with the theoretical results of Tsien and Sowyrda in the linear parts of the shear flow. The experiments show furthermore the sensibility of stalling characteristics and maximum lift of the airfoil to its location in the shear flow. When the product of the local shear and the local derivative of shear is negative, airfoil stall is markedly delayed. When this product is positive, stall is promoted.

Vidal makes some speculations on the possible benefits of the destalling phenomenon in practical applications. He indicates that the wing maximum lift can be augmented by properly orienting the wing with respect to the slipstream of the propeller, that is the wing somewhat below the slipstream axis. He suggests also that a fairly thin shear flow, perhaps comparable in thickness with the airfoil thickness, might suffice to delay stall. This idea is interesting for the tandem airfoil case.

Effects of an airfoil on the flap was investigated by Moser and Shollenberger[7] Oskam, Lean and Volkers[8], Butter[9] and Porcheron and Thibert.[10] These researchers indicate that there is an effect of the total head distribution in the wake of the airfoil on the characteristics of the flap.

Gersten and Gluck[11] investigated the effect of a wing on tail plane, in two-dimensional case. They indicate that this effect may be important when the angle of attack is high. They found that the tail surfaces are exerted an additional lift due to wing wake, like as in Tsien's case.

In the tandem case a limited number of investigations are found in the literature which are only the theoretical approaches. For example, Bairstow[12] and Glauert[13] treated the forces on two airfoils with the chords on the same line, by representing them by two straight lines. Sedov[14] extended the treatment to the case that the second airfoil have an angle with respect to the first one, like a flap. In the recent years Watt and Parkinson[15] made a similar investigation to calculate the effects of angle of attack and flap angle quickly on two element airfoils. All these investigations make thin airfoil assumption and do not contain the thickness, camber and viscosity effects.

In this paper, the lift and pitching moment characteristics of an airfoil are investigated in isolated and tandem case, theoretically for the potential case and experimentally at a Reynolds number of about $6.5\ 10^5$. In the first part, the complex panel method is presented. Second part is devoted to the experimental and theoretical investigations on the airfoil in isolated and tandem cases. Finally, concluding remarks are presented.

Theoretical Method

The panel methods are generally based on Green's third identity, which yields a representation of the potential or the stream function at any point of a potential flow field in terms of a distribution of sources, doublets or vortices along the boundary surfaces. Application of the boundary condition leads to a Fredholm equation of the first or second kind. The panel methods convert this integral equation into a set of linear equations by dividing the boundary surfaces into small elements (panels). There are many panel methods in the literature differing from each other in the kind of singularities used, in the application of the boundary condition and in numerical details.[16,17]

In two-dimensional cases the treatment of a potential problem is easier then in the real plane. Therefore, the complex variables were used by several researchers in the panel method applications in recent years.[18-20] But, there is not an essential starting point in these applications, in order to obtain the integral equations. However, in some integral methods other than the panel methods, the development of the integral equations in the complex plane from Cauchy integral theorem is quite interesting.[21,22]

A panel method in the complex plane is developed, starting from the Cauchy integral theorem. Some details and the early applications of the method are given in ref.23. It is extended for calculating wind tunnel wall effects and a wide variety of applications are presented in ref.24.

Cauchy integral theorem indicates that an analytic function can be evaluated at any point inside a contour in its region of analyticity, once the values of this function are known on the contour. If M number of closed curves are considered in z complex plane, representing a multi-element airfoil system, the unbounded region around these curves can be converted into a simply-connected region by encircling it with a circle of radius R, and by intersecting the closed curves on the circle with M number of barriers (Fig.2). Then the Cauchy integral for an analytic function f(z) is

$$f(z) = f(\infty) + \frac{1}{2\pi i}\int_{\Gamma_c} \frac{f(z_o)}{z_o - z}\, dz_o \qquad (1)$$

Where $f(\infty)$ is the value of integral on the circle when R goes to infinity. z_o represents only the points on the closed

curves, since the integrals on the barriers mutually cancel.

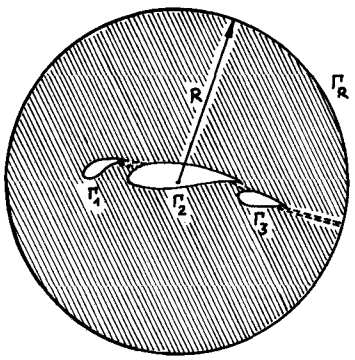

Figure 2 : Simply-connected region

If the complex conjugate velocity is chosen as the analytic function, and the following distribution is taken on the closed curves

$$w^*(z_o) = -i\nu^*(z_o)\cdot t^*(z_o) \qquad (2)$$

where $\nu^*(z_o)$ is a complex singularity

$$\nu^*(z_o) = \sigma(z_o) - i\gamma(z_o) \qquad (3)$$

Then the Cauchy integral gives

$$w^*(z) = w_\infty^* + \frac{1}{2\pi}\int_{\Gamma_c}\left[\frac{\sigma(z_o)}{z-z_o} - i\frac{\gamma(z_o)}{z-z_o}\right]ds \qquad (4)$$

Where ds is the arc length and $t(z_o)$ is the complex representation of the slope of the curve at point z_o defined respectively

$$ds = t^*(z_o)\cdot dz_o \qquad (5)$$

$$t(z_o) = e^{i\delta} \qquad (6)$$

The terms in the integral represent a source and a vortex distribution along the curves, respectively.

Neumann type boundary condition on the curves leads the following integral equation

$$Im\left\{\frac{t(\mu)}{2\pi}\int_{\Gamma_c}\frac{\nu^*(z_o)t^*(z_o)dz_o}{\mu-z_o}\right\} = -Im\{w_\infty^* t(\mu)\} \qquad (7)$$

where μ is the control point on which the boundary condition is applied.

Equation (7) can be written as a sum, by dividing each curves into N_k (k=1,2..M) number of small panels(Fig.3). The panels can be simply chosen as straight lines. If one considers a linear singularity distribution on each element

$$\nu^*(z_o) = \nu_j^* + \nu_j^{*\prime}(z_o-\mu_j)t_j^* \qquad (8)$$

and applies equation (7) for one control point on each element (mid-point of each

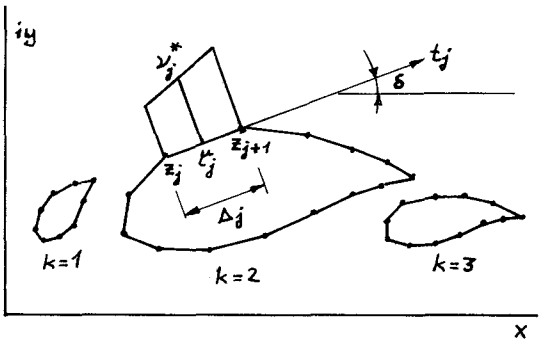

Figure 3 : Panelling

element is chosen in this work), a linear system of equations is obtained with ΣN_k equations

$$\sum_{k=1}^{M}\sum_{j=ni(k)}^{nf(k)} Im\{C_{ij}\nu_j^* + C'_{ij}\nu_j^{*\prime}\} = -Im\{w_\infty^* t_i\}$$
$$(i=1,2,\ldots nf(M)) \qquad (9)$$

where

$$C_{ij} = \begin{cases} -\dfrac{t_i t_j^*}{2\pi} Ln\dfrac{\mu_i - z_{j+1}}{\mu_i - z_j}, & \text{for } i\neq j \\ -i/2, & \text{for } i=j \end{cases} \qquad (10)$$

$$C'_{ij} = C_{ij}(\mu_i-\mu_j)t_j^* - \frac{1}{2\pi}t_i t_j^*\Delta_j$$

The unknown parameter $\nu_j^{*\prime}$ in eqs.(9) can be expressed in terms of the unknowns on the adjacent elements as

$$\nu_j^{*\prime} = e_{1j}\nu_{j-1}^* + e_{2j}\nu_j^* + e_{3j}\nu_{j+1}^* \qquad (11)$$

where

$$e_{1j} = -r/qp, \quad e_{2j} = (r/p - p/r)/q, \quad e_{3j} = p/qr$$
$$p = \Delta_j + \Delta_{j-1}, \quad r = \Delta_j + \Delta_{j+1}, \quad q = -(p+r)/2 \qquad (12)$$

Rearranging eqs.(9) one obtain

$$\sum_{k=1}^{M}\sum_{j=ni(k)}^{nf(k)} Im\{\underline{C}_{ij}\nu_j^*\} = -Im\{w_\infty^* t_i\} \qquad (13)$$
$$(i=1,2,\ldots nf(M))$$

where

$$\underline{C}_{ij} = C_{ij} + C'_{ij-1}e_{3j} - C'_{ij}e_{2j} + C'_{ij+1}e_{1j+1} \qquad (14)$$

Or, defining the real and imaginary parts of $\underline{C}_{ij}$ as a_{ij} and b_{ij} respectively

$$\sum_{k=1}^{M}\sum_{j=ni(k)}^{nf(k)} (b_{ij}\sigma_j - a_{ij}\gamma_j) = Im\{w_\infty^* t_i\} \qquad (15)$$
$$(i=1,2,..nf(M))$$

This equation system contains nf(M) equations for 2*nf(M) unknowns. In order to diminish the number of unknowns, γ_j are taken zero for non-lifting cases. Or, they can be related to a single unknown vortex strength for lifting cases like airfoils

$$\gamma_j = d_j\cdot\gamma_k, \qquad (k=1,2,..M) \qquad (16)$$

by taking a trapezoidal parabolic vortex distribution on each closed surface(Fig.4)

$$d_j = 0.5[\underline{s}_j(\underline{s}_j-1)+\underline{s}_{j+1}(\underline{s}_{j+1}-1)] \qquad (17)$$

Where $\underline{s}_j$ are non-dimensional lengths measured along the curves. Values of γ_k can be prescribed directly, or additional equations are obtained from the Kutta condition for airfoils.

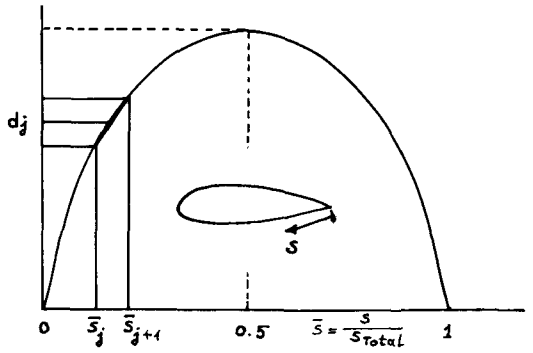

Figure 4 : Trapezoidal parabolic distribution

The solution of eqs.(15) is obtained easily by the Gauss elimination method. The tangential velocities are then obtained by the following relation

$$V_{ti}=Re\{w_\infty^* t_i\} + \sum_{j=1}^{nf(k)} a_{ij}\sigma_j + \sum_{k=1}^{m}\left(\sum_{j=ni(k)}^{nf(k)} b_{ij}d_j\right)\gamma_k$$

$$(i=1,2,..nf(M)) \qquad (18)$$

And the pressure coefficients are calculated from the Bernoulli equation as

$$C_{pi} = 1 - \left(\frac{V_{ti}}{U_\infty}\right)^2, \quad (i=1,2,..nf(M)) \qquad (19)$$

The method outlined above was tested systematically on the Joukowsky and Karman-Trefftz airfoils designed by the method in ref.25. The airfoils had a wide range of thickness and camber ratios changing between 0.05-0.20 and 0.05-0.15 respectively. The obtained results with 50 panels on each airfoil, at 0° and 15° angle of attack are compared with analytical results. Maximum error of lift coefficient is found about 2.5-3% for a camber ratio of 0.15, 1.5-2% for a camber ratio of 0.10 and below 1% for a camber ratio of 0.05 and beyond. The errors decrease generally with increasing thickness ratio.

Another test is carried out to see the effect of number of elements. For a Karman-Trefftz airfoil having a thickness ratio of 0.20 and a camber ratio of 0.15 at 15° angle of attack, the error for lift coefficient is only about 0.7% with 100 surface elements, while this value is about 3% with 50 surface elements.

The method was tested also for the multielement airfoil systems. The agreement with the analytical results were very good for Williams' two-element airfoil[26] and for the four element airfoil of Suddhoo and Hall[27] as seen in Fig.5.

The method can be used for calculating the ground or the wind tunnel wall effects as indicated above. For this type of investigations the ground or wind tunnel walls are represented by straight lines, and divided into small panels. Only a linear source distribution is taken on each panels. And the same calculation procedure is carried out as in the case of multi-element airfoil system. For these calculations, the length of the tunnel walls and the number and the distribution of panels on the walls are important. Therefore, a special investigation must be realized on these parameters before any wall correction calculation.

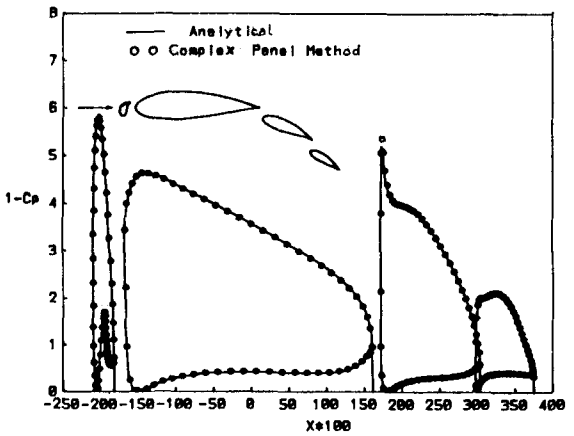

Figure 5 : Four element airfoil

Experimental-Theoretical Investigations in Isolated And Tandem Cases

Experimental Equipment

The experiments were carried out in the low speed, closed circuit wind tunnel of Istanbul Technical University. The tunnel have a 8:1 ratio contraction cone, and a 110 cm wide, 80 cm height, 160 cm length test section. The 44 KW D.C. motor of the tunnel produces velocities in the range of 7-40 m/s in the test section.

The flow quality in the test section was investigated before the experiments on the airfoils. The tests indicate low frequency fluctuations in the velocities up to ±2% of average dynamic pressure. The deviations decrease if an integration is made on the data. For example, if one records the data with an integration time of 30 s the deviation is only ±0.5%. This means that if an integration time is chosen about 20-30 s the uncertainties in the experiments are below 1%.

A second investigation was made on the flow uniformity in the test section. For this purpose, the total and the static pressures were measured in the horizontal mid-section of the testing chamber. The total pressures was found to be uniform over the entire test section. Only small non-uniformities in the entrance and exit

parts of the test section and a little pressure gradient along the test section was observed.

Turbulence level of the flow in the test section was measured by using both turbulence sphere and hot wire anemometer. The turbulence factor was found to be below 1.2 and the turbulence intensity was 0.25%, which corresponds to the measured turbulence factor.

The experiments were realized on the models based on the NACA 65_1 012 airfoil section. The models are made of fiberglass and have a chord of 30 cm. One model was manufactured for the pressure measurements (Model-1), with 47 pressure ports on the mid-span section. Another model is produced for using as the leading airfoil in the tandem case (Model-2). Measured coordinates of models indicate a small deviation from the basic NACA section as seen in Fig.6. Both of the models have an undesired little camber of about 0.3% of the chord. The locations of the pressure tabs on the pressure model are given in Table 1.

The models are mounted in the test section vertically. Thus the chord/height ratio is about 0.27, which is an acceptable value for the airfoil tests in isolated case by using any classical wind tunnel wall correction formulae.

For the pressure measurements a multitube alcohol manometer was used. The liquid levels in the tubes are recorded on the sensible-papers taking place at the background, by using a light source. The time necessary for the record is minimum 1 minute. Thus a natural integration during the record of the data is realized. The height of the columns are measured on the papers. The reading errors are predicted below 1% of the free-stream dynamic pressure, since the dynamic pressure is sufficiently high.

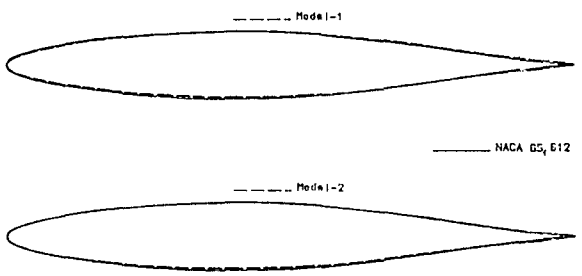

Figure 6 : Models

Results in Isolated Case

The two dimensionality of the flow was observed by using the flow visualization technique by tufts. These tests indicated furthermore that there was a separation bubble near the leading edge of the model at the testing Reynolds number.

Table 1 : Coordinates of the pressure ports on the pressure model

Upper Surface			Lower Surface		
I	X/C	Y/C	I	X/C	Y/C
1	0.0075	0.0081	1	0.0089	-0.0112
2	0.0180	0.0137	2	0.0140	-0.0134
3	0.0280	0.0175	3	0.0226	-0.0168
4	0.0511	0.0240	4	0.0306	-0.0192
5	0.0780	0.0301	5	0.0511	-0.0243
6	0.1013	0.0345	6	0.0753	-0.0295
7	0.1519	0.0425	7	0.1008	-0.0345
8	0.2008	0.0487	8	0.1527	-0.0420
9	0.2513	0.0533	9	0.2032	-0.0476
10	0.3005	0.0565	10	0.2538	-0.0511
11	0.3527	0.0590	11	0.3021	-0.0537
12	0.4043	0.0600	12	0.3513	-0.0555
13	0.4495	0.0597	13	0.4011	-0.0567
14	0.5065	0.0574	14	0.4543	-0.0566
15	0.5548	0.0542	15	0.5027	-0.0549
16	0.6056	0.0499	16	0.5554	-0.0518
17	0.6527	0.0449	17	0.5051	-0.0548
18	0.7043	0.0386	18	0.6546	-0.0428
19	0.7532	0.0316	19	0.7040	-0.0369
20	0.8027	0.0243	20	0.7548	-0.0301
21	0.8540	0.0171	21	0.8032	-0.0234
22	0.9065	0.0113	22	0.8527	-0.0169
23	0.9438	0.0077	23	0.8903	-0.0120
			24	0.9185	-0.0092

In the isolated case, the pressure distribution around the mid-span section of the airfoil model was measured at several angles of attack between -12° and +12° at a flow speed of about 32 m/s and a Reynolds number of about 6.5 10^5. At each angles of attack the lift and pitching moment coefficients were obtained by integrating these pressure distributions. The experiments were repeated individually to see the repeatability. Agreement of the results is very good.

Experimental results were corrected for the wind tunnel wall effects by using the complex panel method. For this purpose, the potential flow characteristics of the model was calculated separately in unlimited flow and in the wind tunnel conditions. For the wind tunnel calculations, the tunnel walls were represented by two straight lines having a length of 40 times the chord of the model, and 20 panels on each wall were considered. Small panel lengths were taken near the model, and the panel lengths were augmented gradually far from the model.

The effectiveness of the panel method was controlled by classical wind tunnel wall correction methods. The calculated lift and pitching moment coefficients in the wind tunnel conditions were corrected for the lift effect by Goldstein's method, and for the blockage effect by Allen, Vincenti and Batchelor's approach.[27] The corrected coefficients were found coincide very good with the results of the panel method in unlimited flow conditions.

For the corrections by panel method, the differences between the coefficients obtained in unlimited flow and in wind tunnel conditions were calculated for each angles of attack, and the following relations were obtained for the differences versus lift coefficients, by using least squares approximation

$$100\,\Delta C_L = 0.0177 - 3.8793\,C_{LT}$$
$$1000\,\Delta C_M = 0.0429 - 4.2711\,C_{LT} \qquad (20)$$

Then the corrections were made by

$$C_L = C_{LT} + \Delta C_L(C_{LT})$$
$$C_M = C_{MT} + \Delta C_M(C_{LT}) \qquad (21)$$

Where C_{LT} and C_{LM} are the measured coefficients.

The corrected lift and pitching moment coefficients of the NACA 65_1 012 based airfoil model at Reynolds number of 6.5 10^5 are presented in Fig.7, together with the potential flow results of the complex panel method for the same model. Both coefficients are nearly linear between -4° and +4° angles of attack. Above these angles the linearity disappears and the airfoil stalls at about 12°. Prompted non-linearity in the coefficients is related possibly to the leading edge separation bubble, which was observed by flow visualization. The theoretical and experimental lift coefficients coincide between 0° and +4° angles of attack. At negative angles of attack the differences between the theoretical and experimental lift coefficients are larger than at positive angles. This is possibly a result of the different characteristic of the leading edge separation bubble on the lower surface, due to camber of the model.

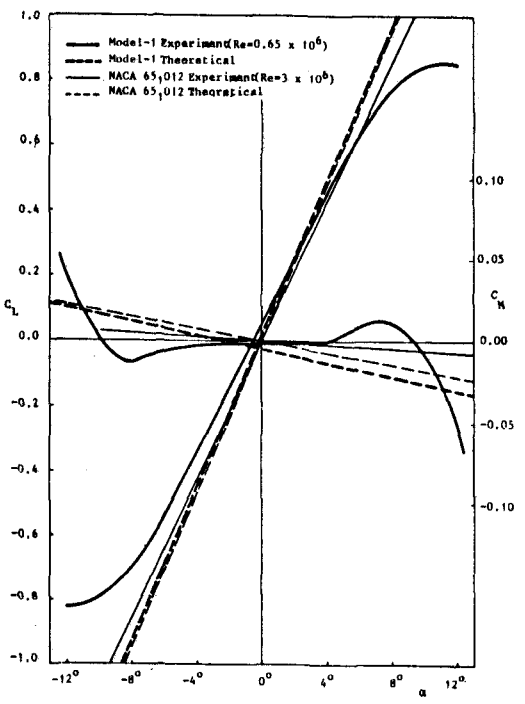

Figure 7 : Lift and pitching moment coefficients in isolated case

Theoretical results and the published experimental results[28] at 3 Million Reynolds number of NACA 65_1 012 airfoil are also presented in Fig.7. There is a small difference between the theoretical coefficients of the NACA airfoil and the pressure model, which is a result of small camber of the model. The difference between the experimental results show the effect of the Reynolds number.

Results in Tandem Case

After the experiments on the NACA 65_1 012 based pressure model (Model-1), a set of experiments in tandem case were carried out by installing the same model in the wake of a similar model (Model-2). The experimental setup is shown schematically in Fig.8. The pressure model is at the center of test section and the other model take place at the upstream. The parameters for these experiments are the distance d between the mid-chord of the models, and the angles of attack of the models, α_1 and α_2. The distance d is chanced by displacing the leading airfoil.

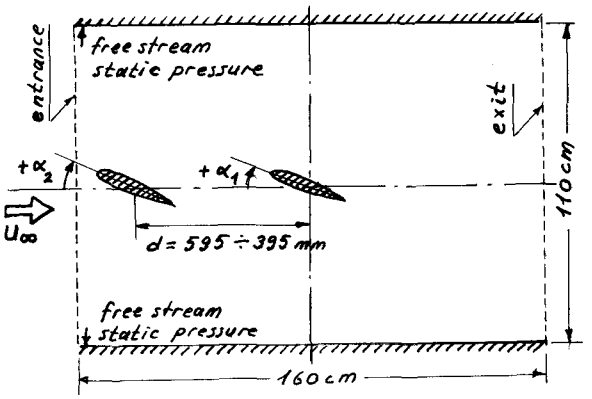

Figure 8 : Experimental setup in Tandem case

At a flow speed of about 32 m/s and a chord based Reynolds number of about 6.5 10^5, the pressure distribution around the mid-span section of the pressure model was measured by the same technique used in isolated case, at several α_1 between -12° and +12°, for the values of d=395, 495 and 595 mm and for the values of α_2=-8°, -4°, 0°, +4° and +8°. Lift and pitching moment coefficients were again obtained by integrating these pressure distributions.

During these experiments, utilization of a pitot-static tube for measuring the free-stream dynamic pressure was not possible, since the testing chamber length is not large enough. Thus the free-stream characteristics were measured on the tunnel walls. The total pressures are taken from the settling chamber walls, and

the static pressure was measured from the testing chamber side walls. Four pressure tabs were located symmetrically on the side walls, near the entrance section, and the average of the pressures taken from these tabs were used for the free-stream static pressure. There was an effect of the models on the static pressure measurements at these points. Thus a correction was needed for these effects.

The effects of the models on the free-stream static pressure measurements and the wind tunnel wall effects were calculated by the complex panel method, and corrected by a procedure developed specifically for the tandem case. For these corrections first the potential flow was calculated around the tandem airfoils both in unlimited flow and in the wind tunnel. Wind tunnel walls were represented again by two straight lines having a length of 40 times the chord, and 40 panels were taken at each wall. The panel lengths were chosen small near the models and gradually augmented far from the models.

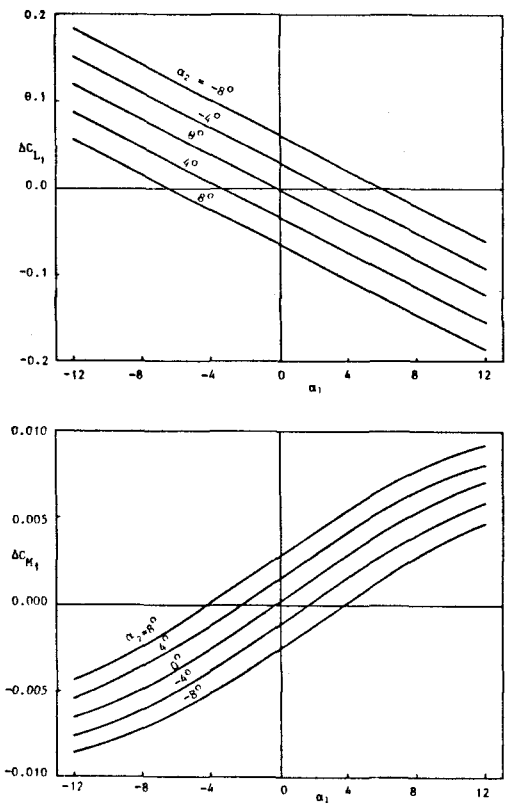

Figure 9 : Wall effects on Model-1 (d=495 mm)

The differences between the values in unlimited-flow and in the wind tunnel conditions of the pressure model's lift and pitching moment coefficients were calculated for each values of the parameters d, α_1 and α_2. As an example, the variations of ΔC_{L_1} and ΔC_{M_1} versus α_1 for d=495 mm are given in Fig.9. The differences for the free-flow static pressures were also calculated in each cases. Variation of ΔC_{p_∞} versus α_1 for d=495 mm is given in Fig.10, as an example.

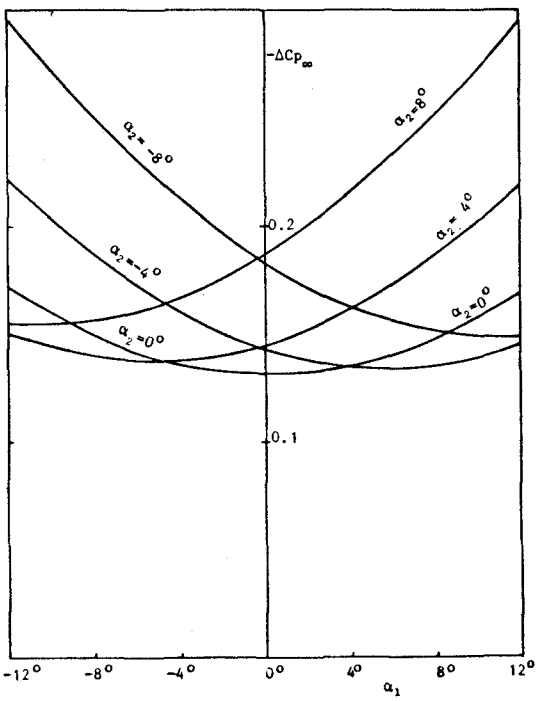

Figure 10 : Model effects on the free-stream static pressure measurements (d=495 mm)

The correction procedure in tandem case is somewhat difficult and different than in isolated case. This is because that the variations of the differences ΔC_{L_1} and ΔC_{M_1} were calculated versus the geometrical angles of attack α_1 and α_2 instead of C_{L_1} and C_{L_2}. At any values of α_1 and α_2 the lift coefficients are lower than the theoretically calculated values due to viscous effects, then the wall effects are also lower than the values predicted theoretically at these geometric angles of attack. Therefore, at any values of α_1 and α_2 first the effective angles of attack were calculated at which the theoretical lift coefficients are the same of the measured coefficients(Fig.11). Then the corrections are realized at these relative angles of attack.

During the experiments, unfortunately, the lift coefficients of Model-2, C_{L_2} were not measured. However, the coordinates and so the theoretical lift coefficients of Model-2 is nearly the same. Thus the experimental characteristics of Model-1 were used for predicting that of the Model-2 for the wall correction purposes only (Fig.12).

Finally the procedure used for the wall corrections is as follows :

i) At any values of α_1 and α_2 the theoretical lift coefficient of Model-2

corresponding its geometrical angle of attack α_2 is predicted from Fig.11, by using the measured lift coefficient of Model-1,

ii) experimental lift coefficient of Model-2 is predicted from Fig.12,

iii) effective angles of attack of both models are found from Fig.11,

iv) then the correction values are obtained from Fig.9 and 10 by using the effective angles of attack,

v) the corrections are made on the measured coefficients of Model-1 by the following relations

$$C_{L1} = C_{L1(measured)}(1-\Delta C_{p\infty}) + \Delta C_{L1}$$
$$C_{M1} = C_{M1(measured)}(1-\Delta C_{p\infty}) + \Delta C_{M1} \qquad (22)$$

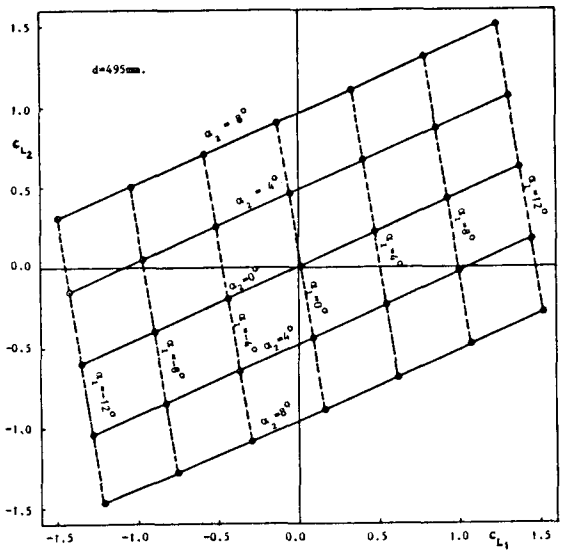

Figure 11 : Relation between the theoretical lift coefficients of Model-1 and Model-2 (d=495 mm)

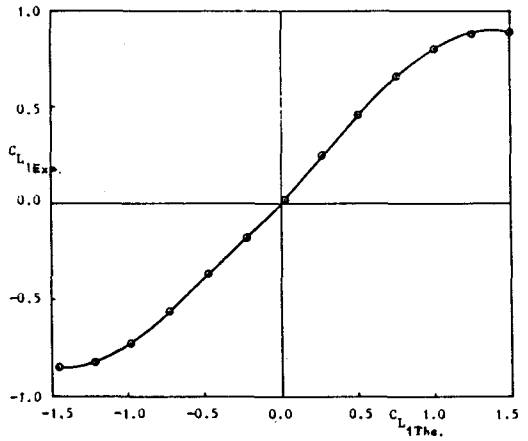

Figure 12 : Relation between the theoretical and experimental lift coefficients of Model-1

Corrected lift and pitching moment coefficients of pressure model in tandem case are presented in Figs.13 a-c, for d=395, 495, 595 mm respectively. The lift and pitching moment-angle of attack of the model in the wake are displaced by some amount depending on the angles of attack of the upstream airfoil, as seen in these figures. These shifts are such that, the coefficients are decrease when the angles of attack of the two airfoils are in the same direction. The coefficients increase when the angles of attack are in the opposite directions.

The theoretical lift and pitching moment coefficients of the pressure model in tandem case obtained by the complex panel method are presented in Figs.14 a-c, for d=395, 495 and 595 mm, respectively. Similar shifts are seen in lift and pitching moment curves of downstream model. This similarity between the theoretical and experimental results points out that the shifts in the coefficients are sourced primarly from the changes in the direction of the flow approaching to the downstream airfoil due to angle of attack of the leading airfoil.

Theoretical and experimental results are compared in Figs.15 a-e, for several values of leading airfoil's angle of attack. For non-zero values of α_2, the differences in the theoretical and the experimental coefficients of thedownstream airfoil are larger than that seen in the isolated case. This discripancy means that there is an extra effect other than the upstream airfoil's angle of attack, which is the effect of the wake of leading airfoil. However it is very difficult to asses the degree of this effect resulting from the turbulence or from the slipstream in the wake, by considering the existing experimental and theoretical results.

The shifts seen on the lift and pitching moment curves of the downstream airfoil decrease as the distance between the airfoils icreases.

The experimental and the theoretical results show that the slopes of the lift-angle of attack curves in the tandem case are lower than that in the isolated case. The slopes of the pitching moment-angle of attack curves are higher in absolute values than that of the isolated airfoil. These discripancies in the tandem case also decrease as the distance between the airfoils increases.

Another important effect in the tandem case is seen on the stalling characteristics of the downstream airfoil. There is a tendency of delay in stall of the downstream airfoil, when the angles of attack of the two airfoils are in the same direction, and a tendency to hasten, when the angles of attack are in the opposite directions. It is possible to say that these tendencies in the stalling

characteristics of the airfoil in the wake also result primarily from the changes in the direction of the flow approaching to the downstream airfoil. However there is a similar tendency of delay in the stall of the downstream airfoil when the leading airfoil has zero angle of attack. This shows that there is an extra effect of the leading airfoil's wake on the stalling characteristics of the downstream airfoil. But, it is difficult again, to asses the degree of this effect resulting from the turbulence or from the slipstream in the wake, by considering the existing experimental and theoretical results.

Conclusions

The lift and pitching moment characteristics of a NACA 65_1 012 based airfoil model was investigated in isolated and tandem cases experimentally at a Reynolds number of about 6.5 10^6 and theoretically in potential flow case.

For the potential flow calculations a complex panel method was developed starting from the Cauchy integral theorem. The method was tested widely in isolated case and for multielement airfoils. This method was used also for correcting the wind tunnel wall effects both in isolated and tandem cases.

In isolated case the lift and pitching moment characteristics of the airfoil were obtained by the pressure measurements. The comparisons made with the complex panel method results and with the experimental

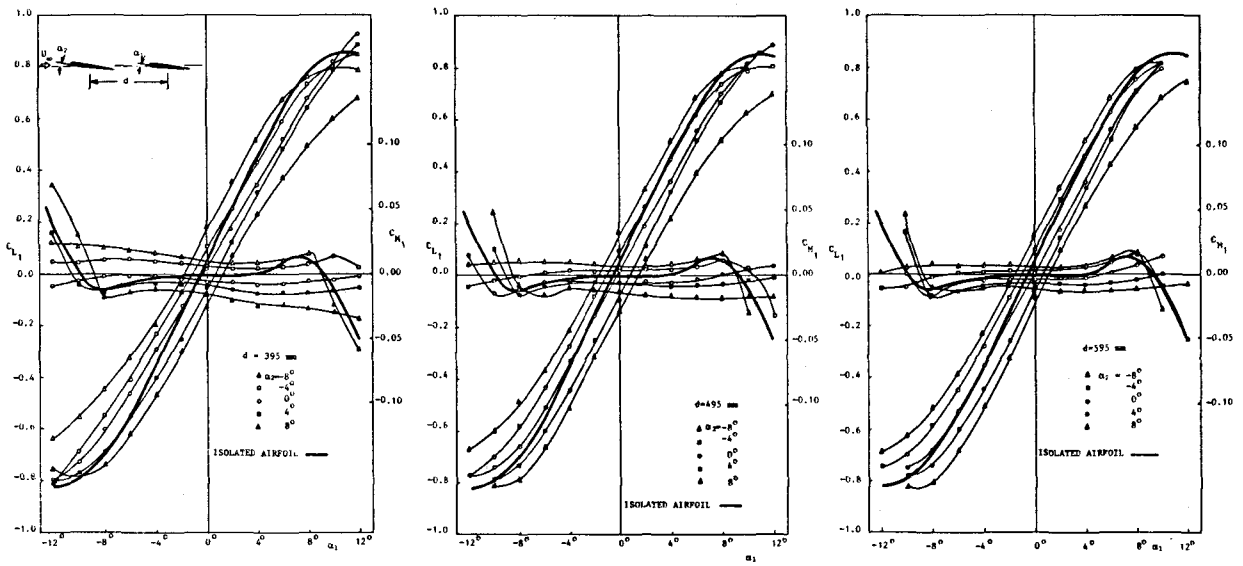

Figure 13 : Corrected experimental characteristics of Model-1 in tandem case

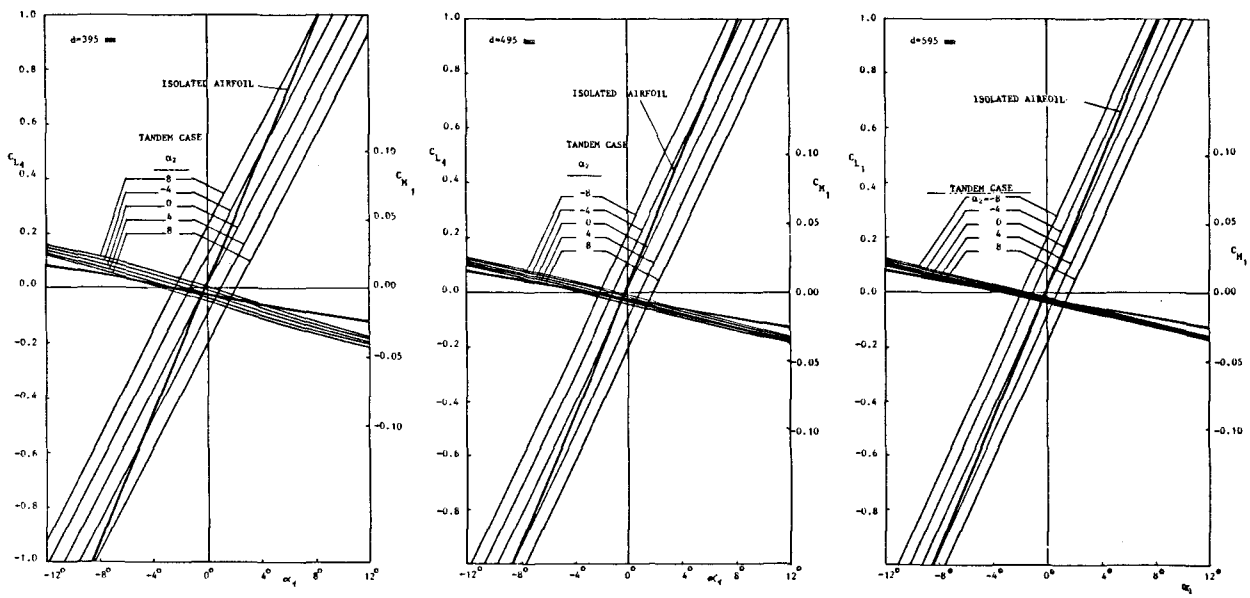

Figure 14 : Theoretical characteristics of Model-1 in tandem case

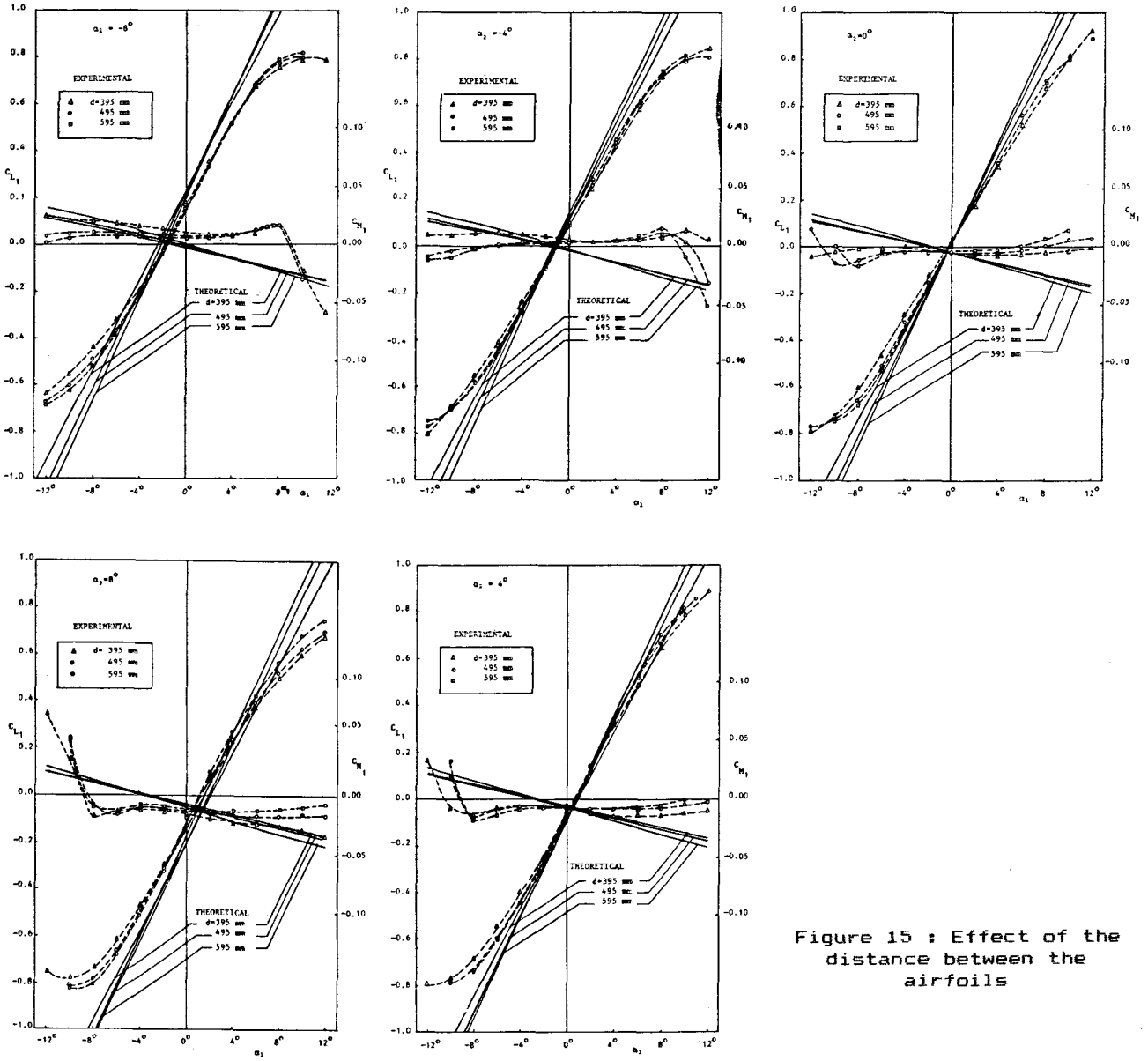

Figure 15 : Effect of the distance between the airfoils

and the theoretical characteristics of the basic NACA airfoil pointed out the viscosity and the Reynolds number effects.

In the tandem case, the lift and pitching moment characteristics of the same model were obtained by the pressure measurements, while it was in the wake of a similar model. Shifts in the lift and pitching moment-angle of attack curves of the airfoil and changes in its stalling characteristics were seen due to primarily changes in the direction of flow approaching to downstream airfoil and furthermore to the wake of the leading airfoil. All these changes decrease with the increasing distance between the airfoils in tandem arrangement.

References

1.Mueller,T.J., "Low Reynolds number vehicles, AGARD-AG-288, 1985.

2.Tsien,H.S., "Symmetrical Joukowsky airfoils in shear flow", The Quarterly of Applied Mechanics, Vol.1, 130-148, 1943.

3.Sowyroda,A., "Theory of cambered Joukowsky airfoils in shear flow", Cornell Aeronautical Lab.Inc.,Rept.AI-1190-A-2 1958.

4.Vidal,R.J., "The influence of two dimensional stream shear on airfoil maximum lift", J. Aerospace Sciences, Vol.29, No.8, 889-904, 1962.

5.Ludwig,G.R. and Erickson,J.C., "Airfoils in two-dimensional non-uniformly sheared slipstreams", J. Aircraft, Vol.8, No.11, 874-880, 1971.

6.Gupta,A.K. and Sharma,S.C., "Cambered Joukowsky airfoil in a nonuniform weak shear flow", J. Aircraft, Vol.11, No.10, 653-656, 1974.

7.Moser,A. and Schollenberger,C.A., "Inviscid wake airfoil interaction on multi-element high lift systems", J. Aircraft, Vol.10, No.12, 765-767, 1973.

8.Oskam,B.; Lean,D.J. and Volkers,D.F., "Recent advances in computational methods to solve the high-lift multi-component airfoil problem", AGARD CP-365, 1984.

9.Butter,D.J., "Recent progress on development an understanding of high lift systems", AGARD CP-365, 1984.

10.Porcheron,B. and Thibert,J.J., "Etude Detaillée de l'écoullement autour d'un profil hypersustente. Comparisons avec les calcules", AGARD CP-365, 1984.

11.Gersten,K. and Gluck,D., "On the effect of wing wake on tail characteristics", AGARD CP-262, 1979.

12.Bairstow,L., "Applied aerodynamics", Longmans, Green and Co., 1946.

13.Glauert,H., "The elements of airfoil and airscrew theory", Cambridge University Press, 1948.

14.Sedov,L.I., "Two-dimensional problems in hydrodynamics and aerodynamics", John Wiley and Sons Inc., 1965.

15.Watt,C.D. and Parkinson,G.V., "On the application of linearized theory to multi-element airfoils, Part.1: Tandem flat airfoils",Aeronautical Quarterly, Vol.34, 46-60, 1983.

16.Hess,J.L., "Review of integral equation techniques for solving potential flow problems with emphasis on the surface source method", Computer methods in applied mechanics and engineering, Vol.5, 145-196, 1975.

17.Bristow,D.R., "Improvements in surface singularity analysis and design methods", NASA CP-1285, 1978.

18.Mokry,M., "Integral equation method for subsonic flow past airfoils in ventilated wind tunnels", AIAA J. Vol.13, No.1, 47-53, 1975.

19.Ojha,J.K. and Shevare,G.R., "Exact solution for wind tunnel interference using the panel method", Computer and Fluids, Vol.13, No.1, 1-14, 1985.

20.Bousquet,J., "Methode des singularités, Théorie et applications", Cours ENSAE, Toulouse, 1982.

21.Hunt,B. and Isaac,L.T., "Integral equation formulation for groundwater flow", J. Hyd. Div. ASCE, HY10, 1197-1209, 1981.

22.Hromadka,T.V. and Guymon,G.L., "A complex variable boundary element method: Development", Int. J. for Num. Methods in Engineering, Vol.20, 25-37, 1984.

23.Yukselen,M.A., "The surface singularity method in complex plane", Proc. Int. Conf. on Computational Mechanics, 1986.

24.Yukselen,M.A., "Investigation of the lift and pitching moment characteristics of an airfoil in tandem arrangement", PhD. Thesis, Istanbul Technical University, 1987.

25.Yukselen,M.A. and Erim,M.Z., "A general iterative method to design Karman-Trefftz and Joukowsky airfoils", Int. J. for Num. Methods in Engineering, Vol.20, No.5, 1349-1368, 1984.

26.Williams,B.R., "An exact test case for the plane potential flow about two adjacent lifting airfoils", A.R.C. R.M. No.3717, 1971.

27.Suddhoo,A. and Hall,I.M., "The test cases for the plane potential flow past multi-element airfoils", Aeronautical J., Vol.89, No.890, 403-414, 1985.

28.Garner,H.C.; Rogers,E.W.E.; Acum,W.E.A. and Maskel,E.C., "Subsonic wind tunnel wall corrections", AGARDograph 109, 1966.

29.Abbott,I.H.; Doenhoff,A.E. and Stivers, L.S., "Summary of airfoil data", NACA Rept.No.824, 1945.